



# Distribution characteristics, source analysis and risk assessment of polycyclic aromatic hydrocarbons in sediments of Kuye River: a river in a typical energy and chemical industry zone

Jinhui Liu · Aining Zhang · Zhuangzhuang Yang · Chunxiao Wei · Lu Yang · Yongjun Liu

Received: 29 July 2023 / Accepted: 8 October 2023 / Published online: 17 February 2024  
© The Author(s), under exclusive licence to Springer Nature B.V. 2024

**Abstract** This study systematically analyzed the distribution characteristics, sources, and ecological risk of polycyclic aromatic hydrocarbons (PAHs) in Kuye River sediments, located in an energy and chemical industry base in northern Shaanxi, China. The results that revealed the concentrations of 16 PAHs in the sediment ranged from 1090.04 to 32,175.68 ng·g<sup>-1</sup> dw, with the four-ring PAHs accounting for the highest proportion. Positive matrix factorization analysis (PMF) revealed the main sources of PAHs as incomplete fossil fuel combustion, biomass combustion, and traffic emissions. The total toxic equivalent concentration of BaP, risk quotient, and lifetime carcinogenic risk of PAHs suggested moderate to high contamination of PAHs in the area. The higher incremental lifetime carcinogenic

risk (ILCR) indicated that PAH ingestion was the primary route of impact on public health, with children potentially being more susceptible to PAH exposure. This study can provide valuable theoretical support for implementing pollution prevention measures and ecological restoration strategies for rivers in energy and chemical industry areas.

**Keywords** Polycyclic aromatic hydrocarbons (PAHs) · Sediment · Distribution characteristics · Source analysis · Risk assessment · Energy and chemical area

## Introduction

Polycyclic aromatic hydrocarbons (PAHs), which are a type of aromatic compounds containing two or more benzene rings, have detrimental effects on human health, including carcinogenic, teratogenic, and mutagenic effect (Han et al., 2021a; Li et al., 2020). PAHs in the natural environment primarily originate from the incomplete combustion of biomass and fossil fuels, and direct emissions from petroleum and its byproducts (Wang et al., 2017). Currently, PAHs are widespread in various environmental media, making them a major global environmental pollution issue (Tepe et al., 2022; Zhang et al., 2021). Owing to their hydrophobic nature and low solubility, PAHs accumulate in water sediments (Chen et al., 2022). Numerous studies have emphasized the threats they

**Supplementary Information** The online version contains supplementary material available at <https://doi.org/10.1007/s10653-023-01802-6>.

J. Liu · A. Zhang (✉) · Z. Yang · C. Wei · L. Yang · Y. Liu  
School of Environmental and Municipal Engineering,  
Xi'an University of Architecture and Technology, Yan Ta  
Road, No.13, Xi'an 710055, China  
e-mail: zhangaining@xauat.edu.cn

Y. Liu  
e-mail: liuyongjun@xauat.edu.cn

J. Liu · A. Zhang · Z. Yang · C. Wei · L. Yang · Y. Liu  
Key Lab of Northwest Water Resource, Environment  
and Ecology, Ministry of Education, Xi'an University  
of Architecture and Technology, Xi'an 710055, China

pose cause to human health and ecosystems (Falciglia et al., 2018; Zeng et al., 2018).

The Kuye River, classified as a first-class tributary of the Yellow River Basin, is located in an energy and chemical industry zone in northern Shaanxi, China. The upper reaches of the Kuye River are home to a significant number of coal mines and coal-processing industrial parks. Energy and chemical enterprises, such as orchid charcoal industrial parks, thermal power plants, coking plants, and oil refining plants, are mainly distributed in the middle reaches. The Shenfu coalfield, one of the seven largest coalfields globally, and China's largest orchid charcoal industrial park are also situated in this region. Consequently, this area has gained recognition as a crucial coal production and national energy chemical base in China. Over time, continuous coal mining, processing, and production by energy and chemical companies have exacerbated the contamination of the river. Among the contaminants found in river sediments, PAHs are a particular concern due owing to their highly toxic nature. However, lots of studies on the rivers in this region have primarily focused on watershed runoff, sand transport, and heavy metal pollution, paying relatively less attention to river sediment pollution, especially the potentially more harmful PAHs pollution (Li et al., 2022; Song et al., 2021). Therefore, it has become essential to evaluate the distribution characteristics, conduct source analysis, and assess the ecological risk of PAHs in the sediments of the Kuye River in the energy and chemical industry area.

In recent years, there has been increasing concern about environmental pollution caused by PAHs owing to their high toxicity and persistence (Kong et al., 2023; Mitra et al., 2019). Sediment is the important destination of PAHs in water bodies (Sharifi et al., 2022). Consequently, the sources of PAHs in river sediments are also receiving more attention. Previous studies have focused on the distribution, sources and risk assessment of PAH contamination in water sediments from urban water systems, estuaries and coastal areas worldwide (refer to Table 2). However, comprehensive studies of PAH contamination in river sediments from typical inland energetic zones are still relatively lacking (Bateni et al., 2022; Dudhagara et al., 2016; Kurwadkar et al., 2022). Past studies have primarily used principal component analysis (PCA) and molecular diagnostic ratio (MDR) to analyse sources

of PAHs in sediments. However, PCA model is susceptible to unexplained factor loadings, and MDR model enables only a qualitative analysis of PAH sources. Therefore, using a single model is insufficient to comprehensively fully analyze the sources of PAHs in sediments. In addition, compared to the PCA model, the positive matrix factorization (PMF) model is more established for source analysis of particulate matter (Li et al., 2014; Salim et al., 2019; Zhang et al., 2020). Therefore, considering the special characteristics of mining energy activities in energy and chemical regions, this study used the PMF model and MDR to analyze the sources of PAHs in sediments. This analysis could provide a theoretical foundation for the development of pollution prevention and control measures for PAHs in river sediments in energy and chemical regions.

In this study, 59 river sediments samples were collected from the Kuye River, and 16 priority PAHs in these samples were detected (Table S1). The objectives of this study were as follows: (1) to systematically analyze the content and distribution characteristics of PAHs in the 59 sediment samples from the Kuye River basin; (2) to perform qualitative and quantitative analysis of the sources of PAHs using molecular diagnostic ratios and PMF models; (3) the total equivalent concentration of BaP ( $TEQ_{BaP}$ ), risk quotient (RQ), and lifetime carcinogenic risk model.

## Materials and methods

### Study area and sampling

In November 2021, surface sediment samples (0–20 cm) were collected at 59 sampling locations within the Shaanxi portion of the Kuye River (Fig. 1). Subsequently, a GPS locator was used to accurately record the locations. Of the sampling points. Specific details about the sampling sites can be found in Table S2. A sampling grid measuring 1 m<sup>2</sup> was established near the midstream channel of the river. After the clearing up of debris, sediment samples were obtained from the four the corners and center of the grid using were collected with a stainless-steel grab sampler. Finally, the sediment was placed in a polyethylene bag and then thoroughly mixed, sealed, and refrigerated.

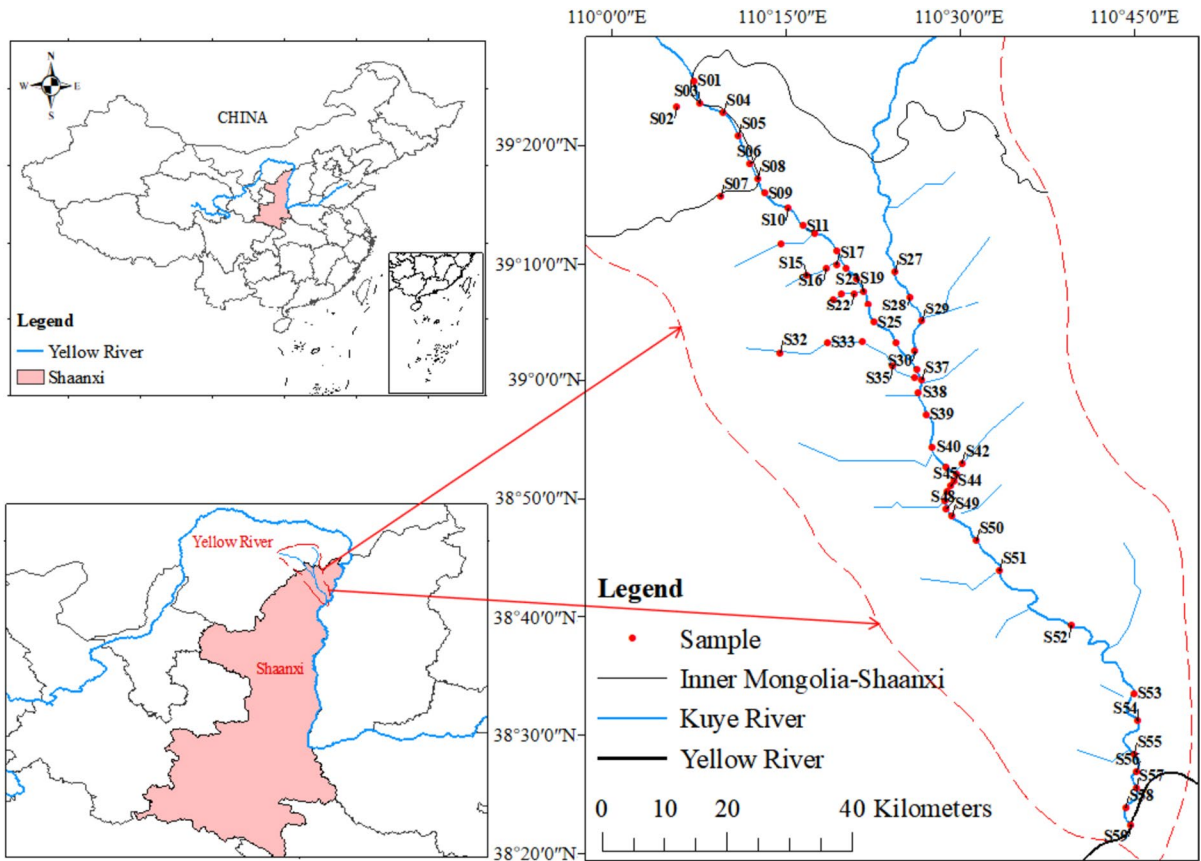


**Fig. 1** Regional location of Kuye River and distribution of sampling points

Extraction and component analysis of PAHs

*Sample processing*

PAHs were extracted according to the previous method (Han et al., 2021b). In summary, a specific amount of the sample was weighed and then fully ground after 24 h of freeze-drying, followed by sieving through a 100-mesh sieve. Subsequently, 1.2 g of activated copper powder, 12.5 mL of n-hexane (C<sub>6</sub>H<sub>14</sub>), and 12.5 mL of dichloromethane (CH<sub>2</sub>Cl<sub>2</sub>) were added (both dichloromethane and n-hexane were of chromatographic grade quality). The mixture underwent ultrasonication for 20 min, and the organic phase was separated through centrifugation. This extraction process was repeated three times using the same procedure, and the resulting organic phases were combined. The mixture was then concentrated to 1 mL using a thermal evaporation sample

concentrator. Next, the concentrated solution was subjected to purification using a purification column (composed of gel, alumina, and anhydrous sodium sulfate). The solution was subsequently eluted with a mixture of 25 mL of n-hexane and 25 mL of dichloromethane. Finally, the mixture was evaporated to complete dryness using a thermal evaporation sample concentrator, and its volume was accurately fixed to 1 mL with n-hexane.

*Program setting of gas chromatography*

The detection of 16 PAHs in 59 sediment samples was conducted using gas chromatography (Agilent 7890a) following the method described by Yang et al. (2022). The HP-5 chromatographic column was chosen for the analysis of PAHs. Nitrogen with a purity greater than 99.999% was used as the carrier gas (flow rate: 1.0 mL/min), and a 1 µL injection volume

was employed during sample analysis. Initially, the oven temperature was set at 80 °C and held for 4 min. Subsequently, it was increased at a constant rate of 8 °C/min to 170 °C, 250 °C, and 300 °C, with each temperature being maintained for 10 min. Finally, the inlet temperature and FID detector temperature were set at 280 °C and 320 °C, respectively, with a splitting ratio of 10:1. The spectrograms of the standard samples are displayed in Fig. S1.

#### Quality assurance/quality control (QA/QC)

To avoid possible interference and cross-contamination, a procedural blank test was performed using the same method as for the sediment samples. Prior to the determination, all sediment samples were spiked with 10 µL of a standard solution containing 16 PAHs. 10 µL of a standard solution containing 16 PAHs was added. The recoveries for the 16 PAHs ranged from 70.2 ± 8% to 104 ± 7%, and the detection limits (MDLs) fell within the range of 0.1 to 0.49 µg/kg dw.

#### Source analysis of PAHs

##### *Molecular diagnostic ratios*

The molecular diagnostic ratio method is a qualitative source analysis approach that leverages the variations in the physical and chemical properties of isomers to determine the origins of PAHs (Pichler et al., 2021). This method has been widely utilized for the qualitative analysis of PAH sources in sediments (Han et al., 2019; Pichler et al., 2021; Yunker et al., 2002). The sources of PAHs associated with different molecular ratios have been documented in numerous studies (Han et al., 2019). In this study, three molecular ratios were calculated: Fla/(Fla + Pyr), Ant/(Ant + Phe), and BaA/(BaA + Chry), to determine the sources of PAHs in the sediments. Table S3 provides an overview of the possible sources of PAHs corresponding to different molecular ratios.

##### *Positive matrix factorization model*

The PMF model is a classical multivariate factor analysis tool developed by Paatero and Tapper in 1994 (Paatero & Tapper, 1994). This method allows for a more precise quantification of the sources and

contribution of PAHs in sediments (Ma et al., 2020). The concentration values of PAHs and their corresponding uncertainties for each sediment sample were input into the model. Calculation of  $X_{ij}$  was performed according to Eq. (1) (Li et al., 2021b; Xu et al., 2016):

$$X_{ij} = \sum_{k=1}^P g_{ik} f_{kj} + e_{ij} \quad (1)$$

$X_{ij}$  denotes the  $j$ th PAH concentration measured in the  $i$ th sample.  $f_{kj}$  is the mass fraction of the  $j$ th PAHs from the  $k$ th source.  $g_{ik}$  is the contribution of the  $k$ th source to the  $i$ th sample, and  $e_{ij}$  is the residue from the  $j$ th source for the  $i$ th sample.

When  $X_{ij}$  is less than MDL, uncertainty ( $\sigma_{ij}$ ) is calculated with Eq. (2):

$$\sigma_{ij} = 5/6 \times \text{MDL} \quad (2)$$

When  $X_{ij}$  is more than MDL,  $\sigma_{ij}$  is calculated with Eq. (3):

$$\sigma_{ij} = \sqrt{(\text{EF} \times x_{ij})^2 + (0.5 \times \text{MDL})^2} \quad (3)$$

where EF denotes the error fraction.

#### Toxicity and ecological risk assessment of PAHs

##### *Equivalent concentration of BaP*

The 16 priority PAHs exhibited varying levels of carcinogenic toxicity, with BaP being the most carcinogenic among them. Consequently, the toxicity equivalence factor (TEF) of BaP served as the standard reference, allowing for the calculation of equivalence factors for the other PAH monomers. The toxic equivalent concentration of PAHs at each location was determined using Formula (4), and the resulting concentration of BaP was recorded as  $\text{TEQ}_{\text{BaP}}$  as shown in Eq. (4) (Li et al., 2021b):

$$\text{TEQ}_{\text{BaP}} = \sum C_i \times \text{TEF}_i \quad (4)$$

$C_i$  denotes the measured concentration of the 16 PAHs, and  $\text{TEF}_i$  denotes the toxicity equivalence factor of the 16 PAHs, as shown in Table S4.

*Risk quotient of PAHs*

The equivalent concentration of BaP provides an overall assessment of PAHs, but does not categorize the risk level. In this study, the risk quotient method—a widely used ecological risk assessment approach, originally proposed by Kalf et al. and modified by Cao et al.—was further used to assess the ecological risk associated with PAHs in the study area (Cao et al., 2010; Kalf et al., 1997). The risk classification criteria can be found in Table S5.  $RQ_{MPCs}$ ,  $RQ_{NCs}$ ,  $RQ_{\Sigma MPCs}$  and  $RQ_{\Sigma NCs}$  were calculated according to Eqs. (5)–(8):

$$RQ_{MPCs} = C_i / C_{QV(MPCs)} \tag{5}$$

$$RQ_{NCs} = C_i / C_{QV(NCs)} \tag{6}$$

$$RQ_{\Sigma MPCs} = \sum_{i=1}^{16} RQ_{i(MPCs)} (RQ_{i(MPCs)} \geq 1) \tag{7}$$

$$RQ_{\Sigma NCs} = \sum_{i=1}^{16} RQ_{i(NCs)} (RQ_{i(NCs)} \geq 1) \tag{8}$$

$C_i$  denotes the concentration of a specific PAH in a sediment sample.  $C_{QV(NCs)}$  and  $C_{QV(MPCs)}$  denote negligible concentrations and maximum permissible concentrations, respectively, as shown in Table S6.

*Human health risk assessment*

The incremental lifetime carcinogenic risk model is a human health assessment method primarily based on BaP, known for its strong carcinogenicity. This model is used to calculate the carcinogenic potential of PAHs in sediment for both children and adults. The risk evaluation criteria for the ILCR model can be found in Table S7 (Wang et al., 2022). The ILCR model suggests that human exposure to carcinogenic substances increases the likelihood of developing cancer (Sharifi et al., 2022). PAHs in sediments can harm humans through three primary routes: skin contact, inhalation and oral ingestion. Dermal contact is the primary route of exposure to PAHs in sediments, followed by oral ingestion and inhalation. The specific calculations for these three carcinogenic pathways

are detailed in Eqs. (9)–(12).  $CS_{BaP}$  represents the BaP equivalent concentration of PAHs in sediments ( $ng \cdot g^{-1}$ ), and the relevant parameters used in these equations are listed in Table S8 (Wang et al., 2022).

$$ILCR_{ing} = \frac{CS_{BaP} \times EF \times ED \times IR}{BW \times AT \times 10^6} \times CSF_0 \tag{9}$$

$$ILCR_{der} = \frac{CS_{BaP} \times EF \times ED \times SA \times AF \times ABS}{BW \times AT \times 10^6} \times \frac{CSF_0}{GIABS} \tag{10}$$

$$ILCR_{inh} = \frac{CS_{BaP} \times EF \times ED \times ET \times IUR}{PEF \times AT} \tag{11}$$

$$ILCR = ILCR_{ing} + ILCR_{der} + ILCR_{inh} \tag{12}$$

Data processing and analysis

The measured PAH concentrations were adjusted with procedural blanks, and data below the detection limit were considered as 0. Data calculations and statistical analyses were performed using Excel 2021. The associated graphs were created using Origin 2021 and ArcGIS 10.8.

**Results and discussion**

Analysis of the levels of PAHs

Table 1 displays the statistical characteristic values and the effects range-low (ERL) and effects range-median (ERM) values for the concentrations of the 16 priority PAHs. The total concentrations of these 16 PAHs ranged from 1090.04 to 32,175.68  $ng \cdot g^{-1}$  dw, with a mean value of 6679.63  $ng \cdot g^{-1}$  dw and a median value of 3775.44  $ng \cdot g^{-1}$  dw. The Table 1 showed that the mean values of all 16 PAHs were higher than the median values. BkF exhibited the highest average concentration (3158.14  $ng \cdot g^{-1}$  dw), followed by BghiP (2765.30  $ng \cdot g^{-1}$  dw) and Pyr (2115.80  $ng \cdot g^{-1}$  dw). In contrast, Nap exhibited the lowest average concentration (81.60  $ng \cdot g^{-1}$  dw). The coefficients of variation for PAHs in these regions were all greater than 0.45 (except for Nap and Chry), with especially high coefficients of variation for Flu, Fla, BkF, and BghiP (coefficient of variation > 1). These results indicate that extreme values were

**Table 1** The content characteristic values and evaluation criteria of PAHs in the study area ( $\text{ng}\cdot\text{g}^{-1}$  dw)

PAHs	Max	Min	Mean	Median	SD	CV	ERL <sup>a</sup>	ERM <sup>b</sup>
Nap	92.20	ND	81.60	84.84	0.01	0.15	160	2100
Ace	2857.72	81.24	641.42	384.84	0.68	0.99	44	640
Flu	2517.64	72.00	267.95	1616.08	0.54	1.56	19	540
Phe	615.56	152.40	315.55	265.80	0.15	0.47	240	1500
Ant	574.64	155.16	273.61	273.40	0.11	0.58	85	1100
Acy	784.36	84.48	198.69	161.80	0.17	0.73	16	500
Pyr	8211.76	714.20	2115.80	1515.36	1.76	0.77	665	2600
Fla	2393.92	131.08	484.61	255.64	0.60	1.06	600	5100
BaA	600.40	97.72	222.73	197.52	0.12	0.50	261	1600
Chry	694.80	134.32	414.97	413.56	0.16	0.36	384	2800
BbF	1969.36	58.48	944.90	745.92	0.66	0.69	320	1880
BaP	1594.96	ND	972.67	916.62	0.45	0.53	430	1600
BkF	7833.60	ND	3158.14	970.24	3.07	1.04	280	1620
DahA	1976.60	743.60	1276.63	1129.80	0.51	0.44	63.4	260
InP	1645.72	33.92	669.29	610.54	0.46	0.64	NA	NA
BghiP	21,228.00	297.44	2765.30	1630.80	4.19	1.24	430	1600
$\Sigma$ PAHs	32,175.68	1090.04	6679.63	3775.44	6.58	0.98	NA	NA

NA not available, ND not detectable

<sup>a</sup>ERL: effects range-low value. (Long et al., 1995)

<sup>b</sup>ERM: effects range-median value. (Long et al., 1995)

present in the study areas. Additionally, the average concentration of high-molecular-weight (HMW) PAHs (PAHs with 4–6 rings) was higher than that of low-molecular-weight (LMW) PAHs (PAHs with 2–3 rings). This phenomenon is attributable to the fact that HMW PAHs are more lipophilic and hydrophobic than LMW PAHs, making them more likely to accumulate in the sediment (Hijosa-Valsero et al., 2016). The higher coefficients of variation suggest a substantial spatial variability in PAH content and pollution levels.

To further assess the pollution level of PAHs in the sediments of the study area, the pollution of PAHs in sediments was classified into four levels through the method introduced by Baumard et al. (1998) (Table S7). Among the sampling sites, ~57.63% were found to have high PAH pollution levels, with PAH concentrations ranging from 1000 to 5000  $\text{ng}\cdot\text{g}^{-1}$  dw. The remaining sampling sites, which experienced heavy PAH pollution, featured PAH concentrations exceeding 5000  $\text{ng}\cdot\text{g}^{-1}$  dw. These results indicate that the area was experiencing high to heavy levels of PAH pollution. The concentrations of PAHs in sediments from the study area were compared with those from other regions around the world (Table 2). Compared with other studies, the levels of PAHs in the Kuye River sediments were significantly higher than those found in the Yellow River, Pearl River, Hai

River, Bahia Blanca Estuary, Clyde River, St. Lawrence, and East Harbor Island. The PAH concentrations in the study area were slightly higher than those in the Yangtze River and Suzhou Industrial Park, while they were somewhat lower than those in the Huaihe River, Forcados River, and Ase River. These results collectively suggest that the concentration of PAHs in the study area is relatively high. Additionally, the ERL and ERM values of Sediment Quality Guidelines (SQGs) were used as evaluation criteria (Table 1). The average concentrations of Nap, Fla, BaA, and BbF were found to be below the ERL, while the DahA and Ace levels exceeded the ERL. The remaining PAHs fell between the ERL and the ERM. The mean concentrations of the carcinogenic PAHs (BaA, Chry, BbF, BkF, DahA, InP, and BaP) exceeded 222.73  $\text{ng}\cdot\text{g}^{-1}$  dw. In summary, the PAH content in the sediments of the Kuye River indicated a moderate to high level of contamination, which poses a serious threat to the ecological environment of the area.

#### Analysis of the spatial distribution of PAHs

The total concentration of PAHs at each sampling site is depicted in Fig. 2. The highest peak concentration of PAHs was observed at site S19 (32,175.68  $\text{ng}\cdot\text{g}^{-1}$  dw), primarily dominated by

**Table 2** Comparison of PAHs in sediments of Kuye River with other locations in the world (ng•g<sup>-1</sup> dw)

Research area	Country	N <sup>a</sup>	Concentration (Mean)	Pollution levels	M <sup>b</sup>	Reference
Pearl River Delta	China	16	69.1 ~ 1297.5(401)	L–H	PCA and MDR	Li et al., (2021a)
Yellow River	China	16	464 ~ 2621(1414)	M–H	PCA and MDR	Xu et al. (2007)
Haihe river	China	16	171.4 ~ 9511.2(2125.4)	M–HE	MDR	Qian et al. (2017)
Yangtze river	China	16	23 ~ 220,000(5500)	L–HE	PMF and PCA	Hong et al. (2022)
Suzhou Industrial Park	China	15	180 ~ 81,000(5700)	M–HE	PMF and MDR	Yuan et al. (2021)
Huai River	China	16	810 ~ 28,228(7955)	M–HE	PCA and MDR	Zhang et al. (2017)
East Harbor Island	USA	14	610 ~ 20,000(3700)	M–HE	PCA and MDR	Neira et al. (2017)
Forcados River	Nigeria	16	1610 ~ 19,800(7870)	H–HE	PCA and MDR	Iwegbue et al. (2021)
Ase River	Nigeria	16	2929 ~ 16,100(7210)	H–HE	PCA and MDR	Iwegbue et al. (2021)
Bahia Blanca Estuary	Argentina	17	19.7 ~ 30,054.5(1798.5)	M–HE	PCA and MDR	Oliva et al. (2015)
Clyde River	Britain	15	2.3 ~ 4226(124)	L–H	MDR	Vane et al. (2017)
St. Lawrence	Canada	16	71 ~ 5672(562)	L–HE	MDR	Corminboeuf et al. (2022)
<b>Kuye River</b>	<b>China</b>	<b>16</b>	<b>1090.04 ~ 32,175.68(6680)</b>	<b>H–HE</b>	<b>PMF and MDR</b>	<b>This study</b>

L low level, M moderate level, H high level, HV very high level

N<sup>a</sup>: Number of PAH compounds analyzed in each study

M<sup>b</sup>: Method of source analysis

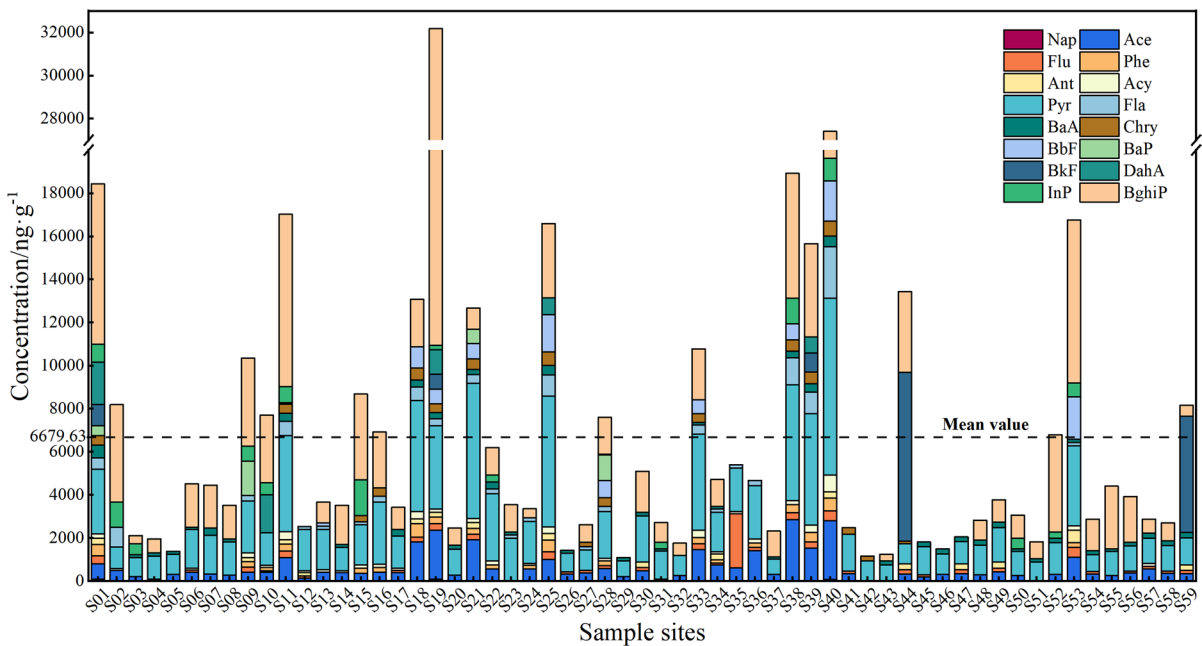


**Fig. 2** PAHs concentrations of various samples in Kuye River

HMW PAHs. The second peak concentration of PAHs occurred in the range of S38–S40 (15,657.84–27,405.92 ng•g<sup>-1</sup> dw). Notably, sediments collected at the junction of the Inner Mongolia section and the Shaanxi section (S01, 18,423.08 ng•g<sup>-1</sup> dw)

exhibited exceptionally high PAH concentrations. Additionally, S09–S11 (ranging from 7695.48 to 17,016.72 ng•g<sup>-1</sup> dw) and S53 (16,746.28 ng•g<sup>-1</sup>) displayed moderate concentrations of PAHs.

These findings align with previous studies, suggesting that the distribution of PAHs is influenced by land use patterns (Yuan et al., 2021). In this study, site S19 was close to industrial areas. The site featured coal enterprises, orchid charcoal enterprises, thermal power plants, and coal-washing facilities. In addition, the concentration of BghiP at S19 is exceptionally higher than that in other regions. It is widely acknowledged that d BghiP are mainly of petroleum origin. In the transport of materials and production processes at local heavy coking industry, large quantities of BghiP can enter the Kuye River sediments through various pathways (Hong et al., 2022). S38 to S40 were situated near Shenmu County, known as the largest coal-producing county in China, and it houses numerous coal mines and coal-processing plants. S01 was close to coal-based energy and chemical companies, coal product manufacturing companies. S09 to S11 were located in Daliuta town at the center of the Shenfu coalfield hinterland. S53 was located in densely populated residential areas. Generally, high concentrations of PAHs are often associated with areas in or near industrial zones (Li et al., 2017).

### Composition analysis of PAHs

PAHs were categorized into three groups according to their ring numbers: two to three rings (Nap, Ace, Flu, Phe, Ant, Acy); four rings (Pyr, Fla, BaA, Chry); and five to six rings (InP, BghiP, DahA, BbF, BaP, BkF), as illustrated in Fig. 3. The concentration of two-to-three-ring PAHs ranged from ND to  $4915.72 \text{ ng}\cdot\text{g}^{-1} \text{ dw}$ , with an average proportion of 15.51%. The content of four-ring PAHs ranged from 811.92 to  $11,787.88 \text{ ng}\cdot\text{g}^{-1} \text{ dw}$ , with an average proportion of 48.69%. The concentration of five-to-six-ring PAHs varied from ND to  $23,948.44 \text{ ng}\cdot\text{g}^{-1} \text{ dw}$ , with an average proportion of 35.80%. The contribution of the three categories of PAHs followed the order of four rings > five to six rings > two to three rings. Since HMW PAHs are more hydrophobic and lipophilic than LMW PAHs, they are typically considered the predominant component of PAHs in sediments (Hijosa-Valsero et al., 2016). The results of this study align with this observation.

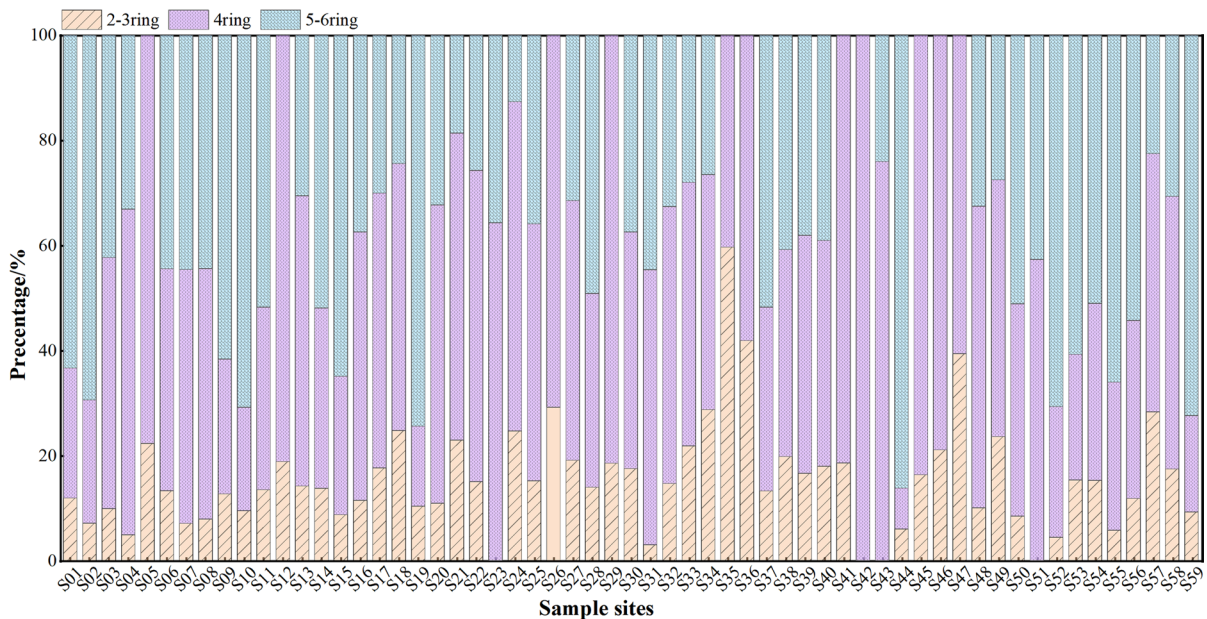


**Fig. 3** Composition of PAHs of various samples in Kuye River



Source identification of PAHs

Molecular diagnostic ratio

Three diagnostic ratios—Fla/(Fla + Pyr), Ant/(Ant + Phe), and BaA/(BaA + Chry)—were employed to determine the sources of PAHs. As depicted in Fig. 4, the molecular ratios of Ant/(Ant + Phe) ranged from 0.27 to 0.72. The Ant/(Ant + Phe) ratios exceeded 0.1 in all sediment samples, suggesting that the combustion of biomass and fossil fuels played a significant role in the PAH sources (Han et al., 2020). The ratios of BaA/(BaA + Chry) fell within the range of 0.22 to 0.57. Twenty percent of the sampling points exhibited BaA/(BaA + Chry) ratios indicative of incomplete petroleum combustion, while the remaining sampling sites exhibited ratios exceeding 0.35, signifying incomplete combustion of coal and biomass sources such as natural gas, fuelwood, and straw as the primary contributors (Han et al., 2020; Yunker et al., 2002). The Fla/(Fla + Pyr) ratios at all sites were below 0.4, suggesting that oil spills were the predominant source (Chen et al., 2022). In summary, the results of this analysis align with land use patterns, indicating that PAHs in sediments likely originated primarily from pyrolytic sources, including coal and biomass combustion, and incomplete petroleum combustion.

Positive matrix factorization analysis

To further quantify the sources of PAHs in sediments and their contributions, the PMF model was utilized. Various numbers of PMF factors ranging from 2 to 6 were selected to ensure that  $Q_{Robust}$  values closely matched  $Q_{True}$ ,  $R^2$  values approached 1, and well-defined factor distributions were obtained. An error fraction of 0.2 was employed. Consequently, the number of factors and the optimal number of iterations were determined as 4 and 36, respectively, and the PMF model iterations yielded favorable results with distinct factor distributions. The outcome of the model operation is presented in Fig. 5. Factor 1 accounted for 29.85% of the total measured PAH concentrations, displaying the highest contribution rate for Fla, followed by Pyr, Chry, and Phe. Fla, Pyr, Chry, and Phe are considered characteristic markers of coal combustion. The profile of factor 1 is similar to that of coal combustion sources (Chen et al., 2022). Therefore, factor 1 is considered the source of coal combustion. Factor 2 accounted for 41.05% of the total PAH concentrations and was primarily associated with BbF, BaP, BkF, DahA, and InP. BbF, BkF, DahA, and InP were identified as markers of incomplete combustion of liquid fossil fuels, and BaP was mainly from coal combustion (Callen et al., 2014). Therefore, factor 2 is considered a mixed source of coal and fossil fuels. Factor 3 accounted for 12.67% of the total measured PAH concentrations, with BghiP being the predominant component. BghiP, an

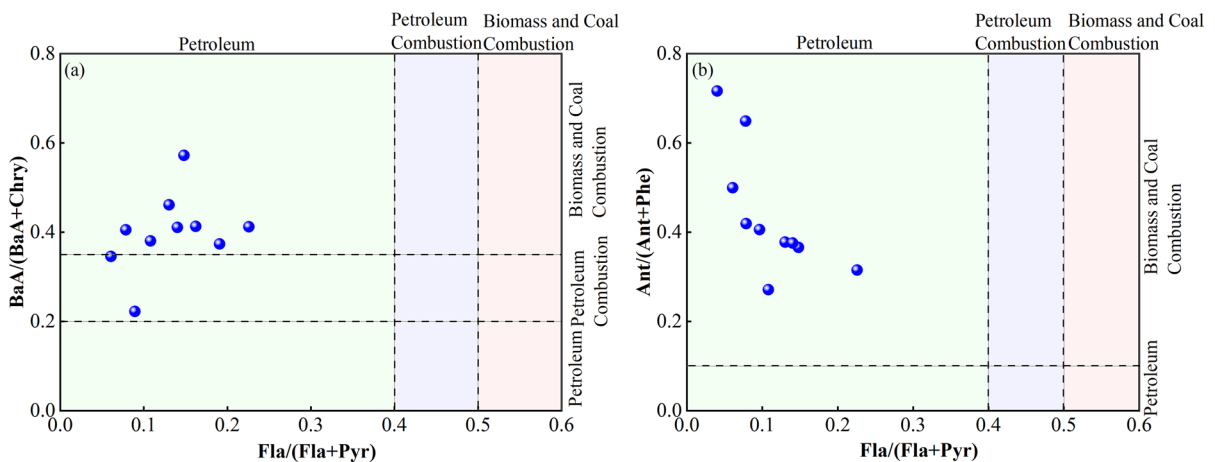
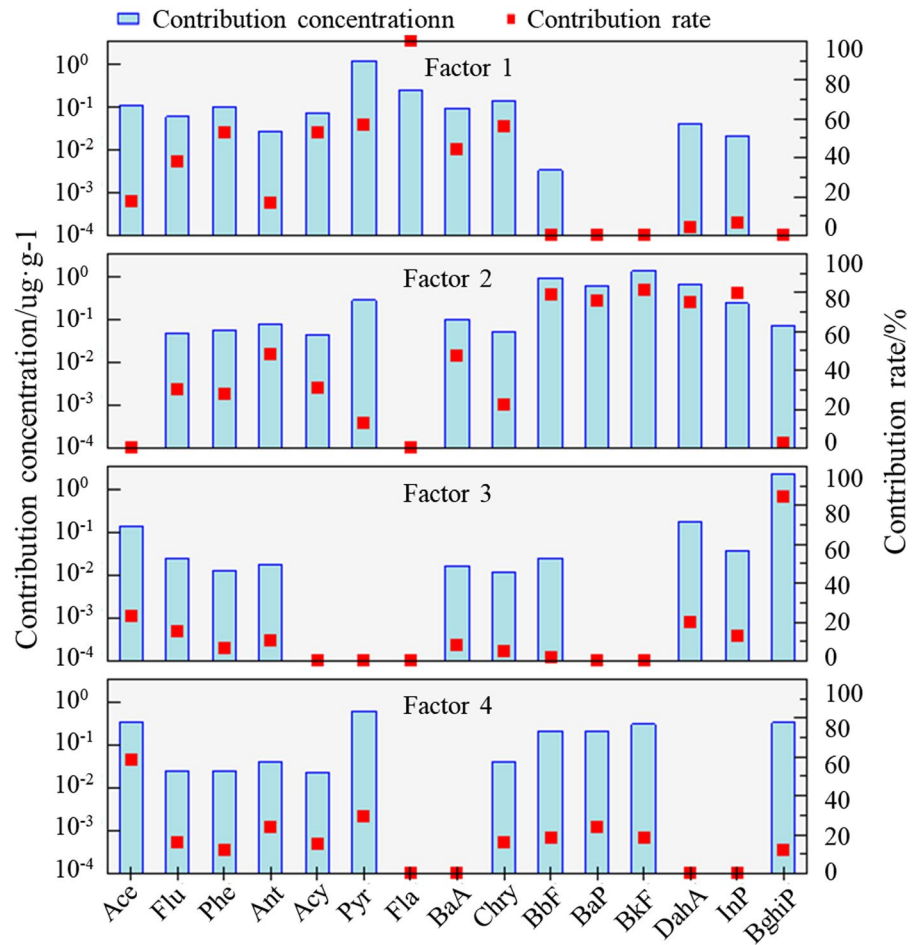


Fig. 4 Molecular diagnostic ratios of PAHs

**Fig. 5** PMF model of PAHs in the sediment

indicator of gasoline combustion, is associated with vehicle emissions (Chen et al., 2022). Hence, factor 3 is reasonably attributed to traffic-related emission sources. Factor 4 contributed 16.43%, with Ace having higher loadings. Ace is recognized as a characteristic product of biomass combustion (Riaz et al., 2019). Factor 4 is therefore identified as a source related to biomass combustion.

The average contribution of each factor, as calculated by the PMF model, reveals that the largest contribution to PAHs in the sediments of the Kuye River was from mixed coal and fossil fuel sources, accounting for 41.05%, followed by coal combustion sources (29.85%); biomass combustion sources contributed 16.43%, and traffic emission sources accounted for 12.67%. The study area is characterized by numerous coal mines and coal chemical industry facilities, along with energy chemical enterprises such as orchid charcoal plants, coking, and oil refining operations.

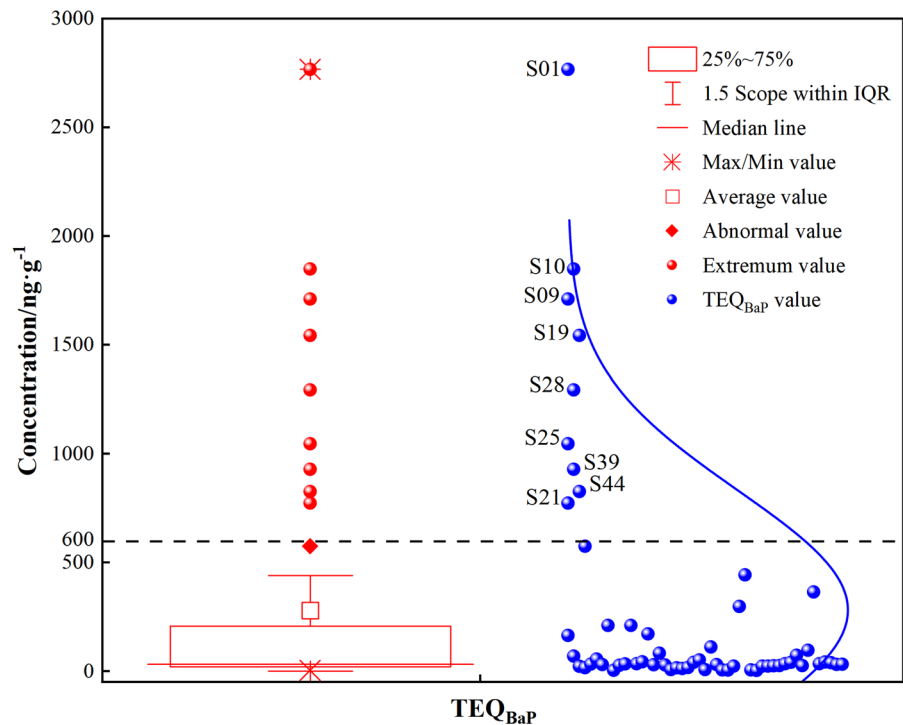
During product processing and transportation, pollutants such as waste liquids and gases can lead to sediment pollution through various pathways. Given the considerable spatial variation in PAH content in the area, it can be inferred that the sediments have been influenced by a range of local industries. In summary, the source analysis results for this typical energy and chemical industry zone align well with the actual situation.

#### Risk assessment of PAHs

##### *Equivalent concentration of BaP*

Figure 6 displays the BaP equivalent concentration ( $TEQ_{BaP}$ ) of the 16 PAHs in the sediment. The  $TEQ_{BaP}$  values in the sediments of all sampling sites in this study ranged from 3.22 (S42) to 2766.33  $ng\cdot g^{-1}$  (S01), with an average of 2280.61  $ng\cdot g^{-1}$ . The

**Fig. 6** Total toxicity equivalence of PAHs in the sediment



TEQ<sub>BaP</sub> of the 7 carcinogenic PAHs varied from 2.04 (S27) to 2683.69 ng·g<sup>-1</sup> (S01), with a mean of 251.06 ng·g<sup>-1</sup>. The highest and lowest TEQ<sub>BaP</sub> values were found at S1 and S42, respectively, which also closely matched the distribution of PAH concentrations. The TEQ<sub>BaP</sub> of the seven carcinogenic PAHs accounted for more than 90% (on average) of the total PAHs. In this study, the TEQ<sub>BaP</sub> evaluation criteria proposed by Environment Canada were selected, and 600 ng·g<sup>-1</sup> was considered a safe toxicity level for PAHs (Wang et al., 2022). A TEQ<sub>BaP</sub> value higher than 600 ng·g<sup>-1</sup> indicates that PAHs in the sediment can have adverse effects on human health. The result showed that TEQ<sub>BaP</sub> exceeded 600 ng·g<sup>-1</sup> at ~15% of the sampling points. Overall, PAHs in the sediments of the Kuye River pose a carcinogenic risk to humans.

*Risk quotient of PAHs*

To further assess the ecological risk posed by PAHs in the sediments of the Kuye River, the RQ method was employed to calculate the RQ<sub>MPCs</sub> and RQ<sub>NCs</sub> values for each sampling point. The calculated results for individual PAHs at each sampling point indicated that the values of RQ<sub>MPCs</sub> (with a mean of 17.63) and RQ<sub>NCs</sub> (with a mean of 1763.16) for Pyr exceeded

1, signifying a high ecological risk. RQ<sub>MPCs</sub> for Ace were also considerably higher than 1 (except for S4 and S31), and RQ<sub>NCs</sub> were all higher than 1, indicating a high ecological risk for Ace. For all other PAH compounds, RQ<sub>NCs</sub> exceeded 1, suggesting a moderate ecological risk for these compounds. Furthermore, the RQ<sub>ΣMPCs</sub> and RQ<sub>ΣNCs</sub> for PAHs were calculated, and the results are presented in Fig. 7. S42, S43, and S51 exhibited RQ<sub>ΣMPCs</sub> values of over 1.0 and RQ<sub>ΣNCs</sub> values of less than 800, indicating a moderate ecological risk for these sites. In contrast, the other sampling points exhibited an RQ<sub>ΣNCs</sub> value of over 800 and an RQ<sub>ΣMPCs</sub> value greater than 1.0, signifying a high ecological risk level. In general, the levels of PAHs in the sediments of the Kuye River indicate a medium to high ecological risk.

*Human health risk assessment*

The results of carcinogenic risk to adults and children from PAHs in sediments, as evaluated by the ILCR model, are presented in Table S9. The ILCR ranges for adults and children were 4.99 × 10<sup>-5</sup>–4.29 × 10<sup>-2</sup> and 3.93 × 10<sup>-4</sup>–3.38 × 10<sup>-1</sup> respectively. According to the adult ILCR results, 8.5% of the sediment samples had ILCR values between 10<sup>-6</sup> and 10<sup>-4</sup>, indicating

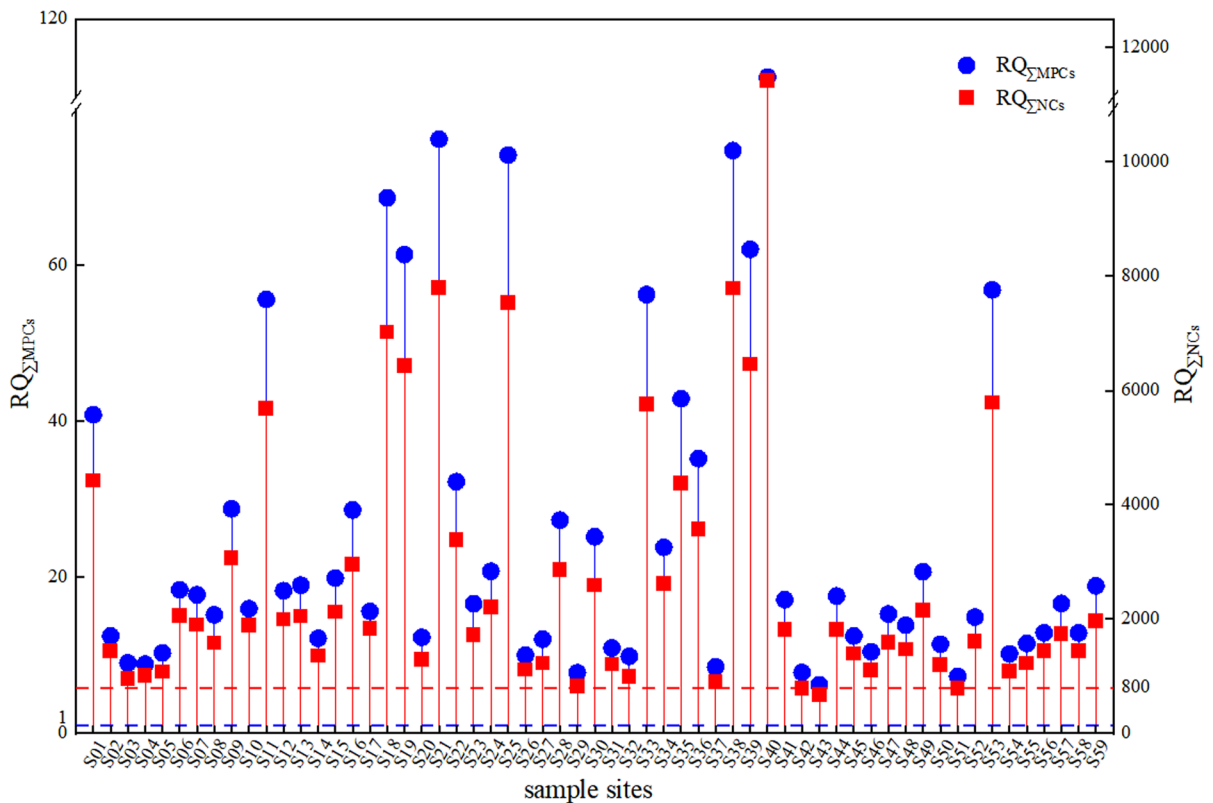


**Fig. 7** Ecological risk quotient of PAHs in the sediment

a low level of carcinogenic risk; 54.24% of the sampling sites had ILCR values between  $10^{-4}$  and  $10^{-3}$ , indicating a moderate level of carcinogenic risk in the area. The remaining sites had ILCR results between  $10^{-3}$  and  $10^{-1}$ , indicating a high risk of carcinogenesis. Regarding the ILCR results for children, 8.5% of the sediment samples had ILCR values between  $10^{-4}$  and  $10^{-3}$ , indicating a moderate level of carcinogenic risk; 74.58% of the sampling sites had ILCR values between  $10^{-3}$  and  $10^{-1}$ , indicating a high level of carcinogenic risk in the area. The remaining sites had ILCR results above  $10^{-1}$ , indicating a very high level of carcinogenic risk (Wang et al., 2022). Overall, the area is characterized by a moderate to high carcinogenic risk. Children are exposed to a higher risk of cancers than adults owing to differences in physical fitness and exposure time (Sharifi et al., 2022). Among the three carcinogenesis routes, the level of carcinogenic risk was highest for the oral cavity, followed by the skin, and then respiration. The risk levels for the oral cavity and skin exposure pathways

were in the same order of magnitude and were much higher than that for the respiration pathway.

## Conclusion

In this study, the distribution characteristics, sources, and ecological risk assessment of PAHs in Kuye River sediments in the energy and chemical industry area were analyzed. The concentrations of PAHs in the Kuye River sediments ranged from 1090.04 to 32,175.68  $\text{ng}\cdot\text{g}^{-1}$  dw, with an average concentration of 3775.44  $\text{ng}\cdot\text{g}^{-1}$  dw. The Kuye River sediments exhibited higher PAH levels than other river sediments, with the main components being HMW PAHs. The spatial distribution results indicated that the PAH pollution in the area was closely related to land use. Additionally, the results of the PMF model and molecular diagnostic ratios suggested that the PAH pollution was due to the incomplete combustion of biomass and fossil fuels and traffic emissions.

According to the toxicity calculations of  $TEQ_{BaP}$  and RQ, the PAHs in the sediments exhibited high biotoxicity and ecological risks, with the potential to cause adverse effects on human health and ecosystems. Furthermore, the lifetime cancer risk model for adults and children in this region yielded values of  $4.35 \times 10^{-3}$  and  $3.43 \times 10^{-2}$ , respectively, indicating that the cancer risk in the area was already high. Therefore, the health risks to the population of the area are currently unacceptable. Furthermore, this study provided a theoretical foundation for implementing pollution prevention and control measures and ecological remediation strategies for PAHs in river sediments in energy and chemical industry areas.

**Acknowledgements** The authors express their gratitude to the reviewers of the manuscript for their valuable comments and suggestions during the review process.

**Author contributions** JHL: Investigation, Visualization, Methodology, Validation, Supervision, Writing—review & editing. ANZ: Investigation, Visualization, Writing—review & editing. ZZY: Investigation, Writing—review & editing. CXW: Visualization, Investigation, Writing—review & editing. LY: Writing—review & editing. YJL: Funding acquisition, Methodology, Writing—review & editing.

**Funding** This research was supported by the National Natural Science Foundation of China, China (Grant No. 51978559), the Key Research and Development Project of Shaanxi Province (Grant No. 2019ZDLSF05-06).

#### Declarations

**Conflict of interest** The authors declare that they have no known competing financial interests or personal relationships that could have appeared to influence the work reported in this paper.

**Ethical approval** All of the investigations were carried out in compliance with the principles of national and international guidelines. Present study does not involve human participants. The manuscript has not been submitted or published in any form, in part or in whole.

**Consent for publication** All of the authors have read and approved the paper for submission of publication.

**Declarations of interest** None.

#### References

- Bateni, F., Mehdinia, A., Lundin, L., & Hashtroudi, M. S. (2022). Distribution, source and ecological risk assessment of polycyclic aromatic hydrocarbons in the sediments of northern part of the Persian Gulf. *Chemosphere*, 295, 133859. <https://doi.org/10.1016/j.chemosphere.2022.133859>
- Baumard, P., Budzinski, H., & Garrigues, P. (1998). Polycyclic aromatic hydrocarbons (PAHs) in sediments and mussels of the western Mediterranean Sea. *Environmental Toxicology and Chemistry: An International Journal*, 17, 765–776. <https://doi.org/10.1002/etc.5620170501>
- Callen, M. S., Iturmendi, A., & López, J. M. (2014). Source apportionment of atmospheric PM<sub>2.5</sub>-bound polycyclic aromatic hydrocarbons by a PMF receptor model. Assessment of potential risk for human health. *Environmental Pollution*, 195, 167–177. <https://doi.org/10.1016/j.envpol.2014.08.025>
- Cao, Z., Liu, J., Luan, Y., Li, Y., Ma, M., Xu, J., & Han, S. (2010). Distribution and ecosystem risk assessment of polycyclic aromatic hydrocarbons in the Luan River, China. *Ecotoxicology*, 19, 827–837. <https://doi.org/10.1007/s10646-010-0464-5>
- Chen, C. F., Ju, Y. R., Lim, Y. C., Wang, M. H., Albarico, F., Chen, C. W., & Dong, C. D. (2022). Potential sources and toxicity risks of polycyclic aromatic hydrocarbons in surface sediments of commercial ports in Taiwan. *Marine Pollution Bulletin*, 181, 113924. <https://doi.org/10.1016/j.marpolbul.2022.113924>
- Corminboeuf, A., Montero-Serrano, J. C., St-Louis, R., Dalpé, A., & Gélinas, Y. (2022). Pre-and post-industrial levels of polycyclic aromatic hydrocarbons in sediments from the Estuary and Gulf of St. Lawrence (eastern Canada). *Marine Pollution Bulletin*, 174, 113219. <https://doi.org/10.1016/j.marpolbul.2021.113219>
- Dudhagara, D. R., Rajpara, R. K., Bhatt, J. K., Gosai, H. B., Sachaniya, B. K., & Dave, B. P. (2016). Distribution, sources and ecological risk assessment of PAHs in historically contaminated surface sediments at Bhavnagar coast, Gujarat, India. *Environmental pollution*, 213, 338–346. <https://doi.org/10.1016/j.envpol.2016.02.030>
- Falciglia, P. P., Catalfo, A., Finocchiaro, G., Vagliasindi, F. G. A., Romano, S., & De Guidi, G. (2018). Microwave heating coupled with UV-A irradiation for PAH removal from highly contaminated marine sediments and subsequent photo-degradation of the generated vaporized organic compounds. *Chemical Engineering Journal*, 334, 172–183. <https://doi.org/10.1016/j.cej.2017.10.041>
- Han, B., Zheng, L., & Lin, F. (2019). Risk assessment and source apportionment of PAHs in surface sediments from Caofeidian Long Island, China. *Marine Pollution Bulletin*, 145, 42–46. <https://doi.org/10.1016/j.marpolbul.2019.05.007>
- Han, B., Liu, A., Wang, S., Lin, F., & Zheng, L. (2020). Concentration level, distribution model, source analysis, and ecological risk assessment of polycyclic aromatic hydrocarbons in sediments from laizhou bay, China. *Marine pollution bulletin*, 150, 110690. <https://doi.org/10.1016/j.marpolbul.2019.110690>
- Han, B., Li, Q., Liu, A., Gong, J., & Zheng, L. (2021a). Polycyclic aromatic hydrocarbon (PAH) distribution in surface sediments from Yazhou Bay of Sanya, South China, and their source and risk assessment. *Marine Pollution Bulletin*, 162, 111800. <https://doi.org/10.1016/j.marpolbul.2020.111800>

- Han, B., Liu, A., Gong, J., Li, Q., He, X., Zhao, J., & Zheng, L. (2021b). Spatial distribution, source analysis, and ecological risk assessment of polycyclic aromatic hydrocarbons (PAHs) in the sediments from rivers emptying into Jiaozhou Bay, China. *Marine Pollution Bulletin*, *168*, 112394. <https://doi.org/10.1016/j.marpolbul.2021.112394>
- Hijosa-Valsero, M., Bécares, E., Fernández-Aláez, C., Fernández-Aláez, M., Mayo, R., & Jiménez, J. J. (2016). Chemical pollution in inland shallow lakes in the Mediterranean region (NW Spain): PAHs, insecticides and herbicides in water and sediments. *Science of the Total Environment*, *544*, 797–810. <https://doi.org/10.1016/j.scitotenv.2015.11.160>
- Hong, S., Kim, Y., Lee, Y., Yoon, S. J., Lee, C., Liu, P., Kwon, B. O., Hu, W., & Khim, J. S. (2022). Distributions and potential sources of traditional and emerging polycyclic aromatic hydrocarbons in sediments from the lower reach of the Yangtze River, China. *Science of the Total Environment*, *815*, 152831. <https://doi.org/10.1016/j.scitotenv.2021.152831>
- Iwegbue, C. M., Irehievwie, G. O., Tesi, G. O., Olisah, C., Nwajei, G. E., & Martincigh, B. S. (2021). Polycyclic aromatic hydrocarbons (PAHs) in surficial sediments from selected rivers in the western Niger Delta of Nigeria: Spatial distribution, sources, and ecological and human health risks. *Marine Pollution Bulletin*, *167*, 112351. <https://doi.org/10.1016/j.marpolbul.2021.112351>
- Kalf, D. F., Crommentuijn, T., & van de Plassche, E. J. (1997). Environmental quality objectives for 10 polycyclic aromatic hydrocarbons (PAHs). *Ecotoxicology and Environmental Safety*, *36*, 89–97. <https://doi.org/10.1006/eesa.1996.1495>
- Kong, J., Ma, T., Cao, X., Li, W., Zhu, F., He, H., Sun, C., Yang, S., Li, S., & Xian, Q. (2023). Occurrence, partition behavior, source and ecological risk assessment of nitro-PAHs in the sediment and water of Taige Canal, China. *Journal of Environmental Sciences*, *124*, 782–793. <https://doi.org/10.1016/j.jes.2022.02.034>
- Kurwadkar, S., Sethi, S. S., Mishra, P., & Ambade, B. (2022). Unregulated discharge of wastewater in the Mahanadi River Basin: Risk evaluation due to occurrence of polycyclic aromatic hydrocarbon in surface water and sediments. *Marine Pollution Bulletin*, *179*, 113686. <https://doi.org/10.1016/j.marpolbul.2022.113686>
- Li, C., Huo, S., Yu, Z., Xi, B., Zeng, X., & Wu, F. (2014). Spatial distribution, potential risk assessment, and source apportionment of polycyclic aromatic hydrocarbons (PAHs) in sediments of Lake Chaohu, China. *Environmental Science and Pollution Research*, *21*, 12028–12039. <https://doi.org/10.1007/s11356-014-3137-8>
- Li, Y., Long, L., Ge, J., Yang, L. X., Cheng, J. J., Sun, L. X., Lu, C., & Yu, X. Y. (2017). Presence, distribution and risk assessment of polycyclic aromatic hydrocarbons in rice-wheat continuous cropping soils close to five industrial parks of Suzhou, China. *Chemosphere*, *184*, 753–761. <https://doi.org/10.1016/j.chemosphere.2017.06.055>
- Li, H., Duan, D., Beckingham, B., Yang, Y., Ran, Y., & Grathwohl, P. (2020). Impact of trophic levels on partitioning and bioaccumulation of polycyclic aromatic hydrocarbons in particulate organic matter and plankton. *Marine Pollution Bulletin*, *160*, 111527. <https://doi.org/10.1016/j.marpolbul.2020.111527>
- Li, H., Lai, Z., Zeng, Y., Gao, Y., Yang, W., Mai, Y., & Wang, C. (2021a). Occurrence, source identification, and ecological risk assessment of polycyclic aromatic hydrocarbons in sediments of the Pearl River Delta, China. *Marine Pollution Bulletin*, *170*, 112666. <https://doi.org/10.1016/j.marpolbul.2021.112666>
- Li, Y., Liu, M., Hou, L., Li, X., Yin, G., Sun, P., Yang, J., Wei, X., He, Y., & Zheng, D. (2021b). Geographical distribution of polycyclic aromatic hydrocarbons in estuarine sediments over China: Human impacts and source apportionment. *Science of the Total Environment*, *768*, 145279. <https://doi.org/10.1016/j.scitotenv.2021.145279>
- Li, X., Liu, X., & Yan, P. (2022). Spatial variability of the physicochemical characteristics of surface sediments in the “Three Rivers and One Dune” Region in the Kuye River Basin, Mu Us Sandy Land, China. *Catena*, *210*, 105943. <https://doi.org/10.1016/j.catena.2021.105943>
- Long, E. R., Macdonald, D. D., Smith, S. L., & Calder, F. D. (1995). Incidence of adverse biological effects within ranges of chemical concentrations in marine and estuarine sediments. *Environmental Management*, *19*, 81–97. <https://doi.org/10.1007/BF02472006>
- Ma, X., Wan, H., Zhou, J., Luo, D., Huang, T., Yang, H., & Huang, C. (2020). Sediment record of polycyclic aromatic hydrocarbons in Dianchi lake, southwest China: Influence of energy structure changes and economic development. *Chemosphere*, *248*, 126015. <https://doi.org/10.1016/j.chemosphere.2020.126015>
- Mitra, S., Corsolini, S., Pozo, K., Audy, O., Sarkar, S. K., & Biswas, J. K. (2019). Characterization, source identification and risk associated with polyaromatic and chlorinated organic contaminants (PAHs, PCBs, PCBzs and OCPs) in the surface sediments of Hooghly estuary, India. *Chemosphere*, *221*, 154–165. <https://doi.org/10.1016/j.chemosphere.2018.12.173>
- Neira, C., Cossaboon, J., Mendoza, G., Hoh, E., & Levin, L. A. (2017). Occurrence and distribution of polycyclic aromatic hydrocarbons in surface sediments of San Diego Bay marinas. *Marine Pollution Bulletin*, *114*(1), 466–479. <https://doi.org/10.1016/j.marpolbul.2016.10.009>
- Oliva, A. L., Quintas, P. Y., La Colla, N. S., Arias, A. H., & Marcovecchio, J. E. (2015). Distribution, sources, and potential ecotoxicological risk of polycyclic aromatic hydrocarbons in surface sediments from Bahía Blanca Estuary, Argentina. *Archives of Environmental Contamination and Toxicology*, *69*, 163–172. <https://doi.org/10.1007/s00244-015-0169-0>
- Paatero, P., & Tapper, U. (1994). Positive matrix factorization: A non-negative factor model with optimal utilization of error estimates of data values. *Environmetrics*, *5*, 111–126. <https://doi.org/10.1002/env.3170050203>
- Pichler, N., de Souza, F. M., Dos Santos, V. F., & Martins, C. C. (2021). Polycyclic aromatic hydrocarbons (PAHs) in sediments of the Amazon coast: Evidence for localized sources in contrast to massive regional biomass burning. *Environmental Pollution*, *268*, 115958. <https://doi.org/10.1016/j.envpol.2020.115958>
- Qian, X., Liang, B., Liu, X., Liu, X., Wang, J., Liu, F., & Cui, B. (2017). Distribution, sources, and ecological risk

- assessment of polycyclic aromatic hydrocarbons in surface sediments from the Haihe River, a typical polluted urban river in Northern China. *Environmental Science and Pollution Research*, 24, 17153–17165. <https://doi.org/10.1007/s11356-017-9378-6>
- Riaz, R., Ali, U., Li, J., Zhang, G., Alam, K., Sweetman, A. J., Jones, K. C., & Malik, R. N. (2019). Assessing the level and sources of Polycyclic Aromatic Hydrocarbons (PAHs) in soil and sediments along Jhelum riverine system of lesser Himalayan region of Pakistan. *Chemosphere*, 216, 640–652. <https://doi.org/10.1016/j.chemosphere.2018.10.139>
- Salim, I., Sajjad, R. U., Paule-Mercado, M. C., Memon, S. A., Lee, B. Y., Sukhbaatar, C., & Lee, C. H. (2019). Comparison of two receptor models PCA-MLR and PMF for source identification and apportionment of pollution carried by runoff from catchment and sub-watershed areas with mixed land cover in South Korea. *Science of the Total Environment*, 663, 764–775. <https://doi.org/10.1016/j.scitotenv.2019.01.377>
- Sharifi, R., Keshavarzifard, M., Sharifinia, M., Zakaria, M. P., Mehr, M. R., Abbasi, S., Yap, C. K., Yousefi, M. R., Masood, N., Magam, S. M., Alkhadher, S. A. A., & Daliri, M. (2022). Source apportionment and health risk assessment of polycyclic aromatic hydrocarbons (PAHs) in the coastal ecosystem of the Brunei Bay, Brunei. *Marine Pollution Bulletin*, 181, 113913. <https://doi.org/10.1016/j.marpolbul.2022.113913>
- Song, J., Yang, Z., Xia, J., & Cheng, D. (2021). The impact of mining-related human activities on runoff in northern Shaanxi, China. *Journal of Hydrology*, 598, 126235. <https://doi.org/10.1016/j.jhydrol.2021.126235>
- Tepe, Y., Aydin, H., Ustaoglu, F., & Kaya, S. (2022). Seasonal distribution and risk assessment of polycyclic aromatic hydrocarbons (PAHs) in surface sediments from the Giresun coast of southeastern Black Sea. *Marine Pollution Bulletin*, 178, 113585. <https://doi.org/10.1016/j.marpolbul.2022.113585>
- Vane, C. H., dos Santos, R. A. L., Kim, A. W., Moss-Hayes, V., Fordyce, F. M., & Bearcock, J. M. (2017). Persistent organic pollutants (PAH, PCB, TPH) in freshwater, urban tributary and estuarine surface sediments of the River Clyde, Scotland, UK. *Earth and Environmental Science Transactions of the Royal Society of Edinburgh*, 108(2–3), 299–313. <https://doi.org/10.1017/s1755691018000294>
- Wang, C., Zou, X., Li, Y., Zhao, Y., Song, Q., & Yu, W. (2017). Pollution levels and risks of polycyclic aromatic hydrocarbons in surface sediments from two typical estuaries in China. *Marine Pollution Bulletin*, 114(2), 917–925. <https://doi.org/10.1016/j.marpolbul.2016.11.027>
- Wang, Z., Liu, Y. J., Yang, L., Yang, Z. Z., Zhang, A. N., Li, Z. H., & Liu, Z. (2022). Distribution, sources, and risk assessment of polycyclic aromatic hydrocarbons (PAHs) in Kaokaowusu river sediments near a coal industrial zone. *Environmental Geochemistry and Health*, 45(9), 6853–6867. <https://doi.org/10.1007/s10653-022-01454-y>
- Xu, J., Yu, Y., Wang, P., Guo, W., Dai, S., & Sun, H. (2007). Polycyclic aromatic hydrocarbons in the surface sediments from Yellow River, China. *Chemosphere*, 67(7), 1408–1414. <https://doi.org/10.1016/j.chemosphere.2006.10.074>
- Xu, J., Peng, X., Guo, C. S., Xu, J., Lin, H. X., Shi, G. L., Lv, J. P., Zhang, Y., Feng, Y. C., & Tysklind, M. (2016). Sediment PAH source apportionment in the Liaohhe River using the ME2 approach: A comparison to the PMF model. *Science of the Total Environment*, 553, 164–171. <https://doi.org/10.1016/j.scitotenv.2016.02.062>
- Yang, L., Liu, Y., Li, C., Liu, Z., Liu, X., Wei, C., Yang, Z., & Zhang, A. (2022). Biodegradation time series characteristics and metabolic fate of different aromatic compounds in the biochemical treatment process of coal chemical wastewater. *Bioresource Technology*, 361, 127688. <https://doi.org/10.1016/j.biortech.2022.127688>
- Yuan, Z., He, B., Wu, X., Simonich, S. L. M., Liu, H., Fu, J., Chen, A., Liu, H., & Wang, Q. (2021). Polycyclic aromatic hydrocarbons (PAHs) in urban stream sediments of Suzhou Industrial Park, an emerging eco-industrial park in China: Occurrence, sources and potential risk. *Ecotoxicology and Environmental Safety*, 214, 112095. <https://doi.org/10.1016/j.ecoenv.2021.112095>
- Yunker, M. B., Macdonald, R. W., Vingarzan, R., Mitchell, R. H., Goyette, D., & Sylvestre, S. (2002). PAHs in the Fraser River basin: A critical appraisal of PAH ratios as indicators of PAH source and composition. *Organic Geochemistry*, 33(4), 489–515. [https://doi.org/10.1016/S0146-6380\(02\)00002-5](https://doi.org/10.1016/S0146-6380(02)00002-5)
- Zeng, Q., Jeppesen, E., Gu, X., Mao, Z., & Chen, H. (2018). Distribution, fate and risk assessment of PAHs in water and sediments from an aquaculture-and shipping-impacted subtropical lake, China. *Chemosphere*, 201, 612–620. <https://doi.org/10.1016/j.chemosphere.2018.03.031>
- Zhang, J., Liu, G., Wang, R., & Huang, H. (2017). Polycyclic aromatic hydrocarbons in the water-SPM-sediment system from the middle reaches of Huai River, China: Distribution, partitioning, origin tracing and ecological risk assessment. *Environmental Pollution*, 230, 61–71. <https://doi.org/10.1016/j.envpol.2017.06.012>
- Zhang, H., Cheng, S., Li, H., Fu, K., & Xu, Y. (2020). Groundwater pollution source identification and apportionment using PMF and PCA-APCA-MLR receptor models in a typical mixed land-use area in Southwestern China. *Science of the Total Environment*, 741, 140383. <https://doi.org/10.1016/j.scitotenv.2020.140383>
- Zhang, R., Han, M., Yu, K., Kang, Y., Wang, Y., Huang, X., Li, J., & Yang, Y. (2021). Distribution, fate and sources of polycyclic aromatic hydrocarbons (PAHs) in atmosphere and surface water of multiple coral reef regions from the South China Sea: A case study in spring-summer. *Journal of hazardous materials*, 412, 125214. <https://doi.org/10.1016/j.jhazmat.2021.125214>

**Publisher's Note** Springer Nature remains neutral with regard to jurisdictional claims in published maps and institutional affiliations.

Springer Nature or its licensor (e.g. a society or other partner) holds exclusive rights to this article under a publishing agreement with the author(s) or other rightsholder(s); author self-archiving of the accepted manuscript version of this article is solely governed by the terms of such publishing agreement and applicable law.